# Rice stem lodging properties and bending modeling under the influence of circadian temperature difference

Bangzhui Wang[1], Zhong Tang[1*], Liyun Lao[2], Guoqiang Wang[3], Tiantian Jing[1], Yao Yu[1]

(1. *School of Agricultural Engineering, Jiangsu University, Zhenjiang 212013, Jiangsu, China*;
2. *School of Water, Energy and Environment, Cranfield University, MK43 0AL, UK*;
3. *Department of Agricultural Engineering, Jiangsu Agriculture & Animal Husbandry Science and Technology Vocational College, Taizhou 225300, Jiangsu, China*)

**Abstract:** Under diurnal temperature stress, the vascular bundle content of mature rice stems will change which will cause a change in the modulus of elasticity. Therefore, the rice stems will collapse with the reduction in bending resistance because of the change in the modulus of elasticity. In order to reveal the distribution of vascular bundle gradients in rice stems under different climatic temperatures and explore the locations where stems are prone to bending and the form of stem damage, this study established a model of stem stiffness under free loading based on observing microstructure of the rice. The lodging characteristics of rice stems was explored seldom in different environmental temperatures from a micro structure of rice stems. So, the statistical analysis and *t*-tests were carried out on stems 1 to 4 in combination for cantilever bending tests at room temperature on stem internodes 3, versus three-point bending tests at –10°C to 65°C temperature treatment. Results showed that the bending resistance of the stem can be well predicted by using the vascular bundle distribution regression model and the variable stiffness mechanical model. The bending resistance of No. 3 stem was established by using the results obtained from the three-point bending test in a temperature range between 10°C-65°C. The correction coefficient TF of stem bending resistance under temperature difference induced stress was established based on the Gauss regression model. Statistical analysis showed that the bending resistance of No.3 stem was relatively large in a temperature range of 16°C-34°C. This study elucidated the variations of the mechanical properties of rice stems under temperature difference induced stress and provided a theoretical foundation for understanding the lodging characteristics of rice during mechanized harvesting.

**Keywords:** rice stem, vascular gradient, stiffness model, stem bending, temperature stress
**DOI:** 10.25165/j.ijabe.20241703.8585

**Citation:** Wang B Z, Tang Z, Lao L Y, Wang G Q, Jing T T, Yu Y. Rice stem lodging properties and bending modeling under the influence of circadian temperature difference. Int J Agric & Biol Eng, 2024; 17(3): 21–32.

## 1 Introduction

Rice is an important food crop in the world, its production is of great significance for the development of human life[1,2]. As a large rice-producing country, China is the largest producer of rice in the world, accounting for approximately half of the global production annually[3]. At present, rice is mainly harvested by combine harvesters[4,5], but harvesting temperature and environmental conditions have an important impact on rice yield[6,7]. Therefore, to ensure an efficient mechanical harvest of rice, it is of great significance to establish a suitable harvest scheduling scheme for combine harvesters based on the mechanical model and growth environment of rice[8,9].

The mechanical properties of the stem directly can reflect its lodging resistance[10]. At present, the primary parameter used for the evaluation of the lodging resistance of the stem is the lodging index. Higher lodging index indicates the rice stem is more prone to overloading. Three types of lodging, including bending, setback and torsion, occur under the condition of lodging, which seriously reduces the working efficiency of combine harvester[11-14]. As shown in Figure 1, the lodging of mature rice will reduce the operational smoothness of the cutting and feeding device of the combine harvester, which will reduce the yield seriously.

The mechanical properties of the lower internodes (1-3) at the base play a crucial role in determining the characteristics of rice stems[15]. Building on this foundation, Luo et al.[16] conducted an analysis and modeling of the 2nd stem at the base under room temperature conditions. Optimal parameters of stem bending resistance were established, and then the lodging index for mature stems evaluated and predicted. However, Li et al.[17] proposed a relative stem wall thickness model, which used the ratio of stem internode wall thickness to its diameter to describe the mechanical properties of stem bending resistance, which seriously affected the mechanized harvesting of rice. Combined with the growth environment of mature rice, Ma et al.[18] found that the mechanical indicators such as the friction coefficient of mature rice stems are larger in high temperature environment, which will affect the mechanical harvesting efficiency. High temperature or low temperature stress has a significant impact on the mechanical properties of stems[19-21], which will affect the final yield of rice further. Therefore, the simulation statistics of the mechanical properties of mature rice stems at different temperatures can ensure

**Received date:** 2023-10-15 **Accepted date:** 2024-04-28
**Biographies: Bangzhui Wang**, Postgraduate, research interest: intelligent harvesting machinery, Email: 656358008@qq.com; **Liyun Lao**, Engineer, research interest: intelligent harvesting machinery, Email: l.lao@cranfield.ac.uk; **Guoqiang Wang**, Engineer, research interest: intelligent harvesting machinery, Email: 474020300@qq.com; **Tiantian Jing**, Postgraduate, research interest: intelligent harvesting machinery, Email: 3143231562@qq.com; **Yao Yu**, Postgraduate, research interest: intelligent harvesting machinery, Email: 3156177253@qq.com.
***Corresponding author: Zhong Tang**, Professor, research interests: agricultural mechanization engineering, Jiangsu university, China. Tel: +86-511-88797338, Email: tangzhong2012@126.com.

the normal harvesting and operation of the harvester, thereby reducing the mechanical harvesting loss of rice.


Figure 1 Rice lodging affects mechanized harvesting

From microscopic view, the content and distribution of vascular bundles of rice stems are important factors affecting the mechanical properties of the stem base[22]. The microstructure of rice stems has distinct layers and has many functions to maintain stem life activities and resist external loads[23,24]. Meng et al.[25] sampled and analyzed different varieties of rice and found that the morphological distribution characteristics such as vascular bundle filling and number have an important impact on the mechanical properties of stems, Gong et al.[26] designed a biomimetic porous sandwich structure similar to the structure of rice stems based on the good compressibility and recoverability of the vascular bundles of stem microstructures; The study from Chen et al.[27] showed that the quantity of small vascular bundles is the primary factor affecting the lodging resistance of rice, and it exhibited a strong positive correlation with the maximum bending resistance of the stem. Consequently, by establishing the pattern of vascular bundle distribution within the stem, one can make preliminary predictions regarding the mechanical properties of the stem and can develop efficient harvesting techniques.

The mechanical properties of stems are to be determined by taking into account a comprehensive understanding of both material mechanics and elastic-plastic mechanics. Huang et al. derived relevant equations for the transverse loaded deformation of the stem, but the calculation is large and not representative. Berry, with a test method for lodging resistance, established a theoretical analysis model for lodging of oat stems and pointed out that different crops have different lodging methods[28,29]. Teng et al.[30] established a unified criterion for the identification and evaluation of resistance to overturning by considering factors such as spike traits, physical strength at the base of the stem and root morphology. A lot of research has been done on the bending model of rice stems. Wu et al.[31] used a high-throughput micro-CT-RGB imaging system and deep learning (SegNet) technology to establish a damage-free quantitative rice bending moment model[32,33] proposed a rice yield classification model based on visual algorithm processing to quantify the lodging resistance of stems. The mechanical properties of stems in the above studies mostly is based on simulated loading, and the studies on the calculation of stiffness or bending modulus, based on the deformation of stems in the real state, are unfrequent. Moreover, the above research cannot give the weak position of the stem on freely loaded and predict the lodging behavior of mature rice.

Therefore, this study established a regression model to reveal the distribution of vascular bundles based on the functional gradient of rice stem microstructure. In order to predict the easy lodging position of the stem by combining with the stiffness mechanical model, cantilever bending tests and the three-point bending tests at a temperature range of –10°C to 65°C were further carried out to analyze the susceptibility of stalks to collapse under different temperature stresses and the magnitude of the collapse force. The correction coefficients of the stem bending force under different temperature stress were derived, and a numerical method for predicting the stem bending stiffness and bending force based on the mechanical model was established. The findings can provide a certain theoretical foundation for the mechanized harvesting of rice and contribute to the reduction of harvest losses.

## 2 Material and methods

### 2.1 Characteristics of mature rice

The raw materials used in this experiment were the ear-picking rice of Huaidao No. 10 in the Jiangsu region of China (116°18′E-121°57′E, 30°45′N-35°20′N). The rice has moderate plant height, compact plant type, erect leaves, and strong lodging resistance. In this experiment, the rice plants were harvested manually after they were mature, and the plants with good growth conditions, full grains, and no pests and diseases were selected as the test samples, (accuracy of 1 cm), electronic scales (accuracy of 0.1 g), etc. to measure the physical structure parameters of the plant, as shown in Figure 2.

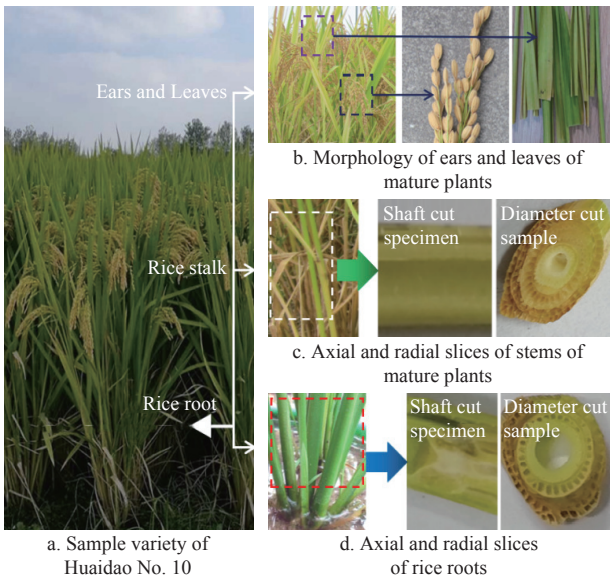


Figure 2 Morphological features and structures of various parts of rice plants

Mature rice straw is at an angle of about 15°-30° to the ground, with a thousand-grain weight of about 28 g, a total number of 110-130 grains per spike, and a fertility rate of 90%-95%. The average height of the rice used in the experiment was about 850 mm. The length of the cut rice straw was about 700 mm. The diameter of the

rice straw roots was about 7 mm. The moisture content of 10 rice straw samples was measured and the average value was taken to be 60.2% at the root of the rice straw and 49.7% at the top of the rice straw.

### 2.2 Microstructure observation test and analysis

In order to observe the microstructure of rice, the WN25VY photo platinum electron microscope of China New Bell Technology Co., Ltd. was used to observe the microscopic morphology of rice stems before and after threshing. The magnification test can reach ×2000. Complete unbroken stems and rice leaves were selected as test samples for cutting and grouping, and the samples were observed with a combination of ×60 eyepiece and ×10 objective lens.

The rice leaves, stems, etc. were supported on the microscope stage, and the resulting images were displayed on the display screen matched with the test, as shown in Figure 3.

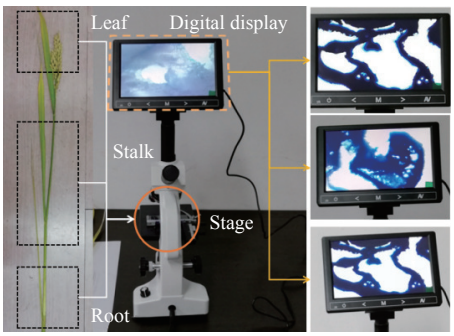


Figure 3 Optical platinum electron microscope

The image of the microstructure can be stored on the PC through the interface. After completing the measurement of stem tissue, the vascular bundle layer was gray-scaled, the number and distribution area of vascular bundles were calibrated and counted, and the relationship between the number and area of vascular bundles and plant stiffness was obtained by further analysis of variance.

### 2.3 Rice stem variable stiffness mechanical model

The mechanical properties of rice against bending are mainly determined by the density of vascular bundles and epidermal mechanical tissue layers in rice stems[34]. In order to reveal the mechanical model and stability of rice stem under different conditions, a stem model is established based on material mechanics, and designed lateral and longitudinal loading to simulate the bending model of naturally loaded rice. In order to simplify the calculation model, this paper makes the following assumptions:

1) In the radially compressed condition, the stalk partly bends and the rice stalk nodes do not change significantly[35], so the change in force at the rice stalk nodes is neglected;

2) The cross section of the stem is a highly symmetrical circular ring[36];

3) Based on the microstructure observation test of rice stalks, it can be obtained that the stiffness of rice stalks has a gradient distribution, and the mechanical properties show a linear trend from bottom to top.

First, this study established the static parameters of the stem, including the length and diameter of each segment of the stem. Regarding the establishment of the stem model, this study is based on the following Equation (1), and the label is $i$ ($i$=1, 2, 3, ..., $n$) from the bottom up. Among them, the length of the stem and its internodes has a power function relationship, and the established stem length is:

$$l_i = \frac{l_0}{\max\limits_{\sum_{i=1} l_i}} l \tag{1}$$

where, $l_i$ is the length of the $i$-th internode, mm; $l$ is the total length of stem plant, mm; $l_0$ is the relative stem length, mm; it can be solved by the following Equation (2):

$$l_0 = ai^b \tag{2}$$

where, $a$ is the internode length coefficient of the stem, 80.36, $b$ is the internode length index of the stem, –0.6657, and the diameter of the stem has an exponential relationship with its position, which can be solved by Equation (3):

$$d_i = \frac{l_i}{a' l^{b'}} \tag{3}$$

where, $d_i$ is the diameter of the $i$-th internode, mm; $a'$ is the internode diameter coefficient, 594.2; $b'$ is the internode diameter index, –0.2362; The difference calculation method detects the conformity of the model, as follows:

$$R_0 = \sqrt{\frac{\max\limits_{\sum_{i=1}} (x_i - x_t)^2}{n}} \tag{4}$$

where, $x_i$ is the predicted value of the model, mm; $x_t$ is the actual parameter of the stem, mm; $n$ is the sample size; calculated the $R_0$ values of the stem length and position variation model, stem diameter and position variation model are 2.67%, 3.69%.

The length of the $i$-th internode, based on the three assumptions, was obtained in the above calculation process. And then, the formula of the relation between diameter and position was obtained and the conformity of the model verified by the difference calculation method. After solving the morphological parameters of the stem, a model is established, as shown in Figure 4.

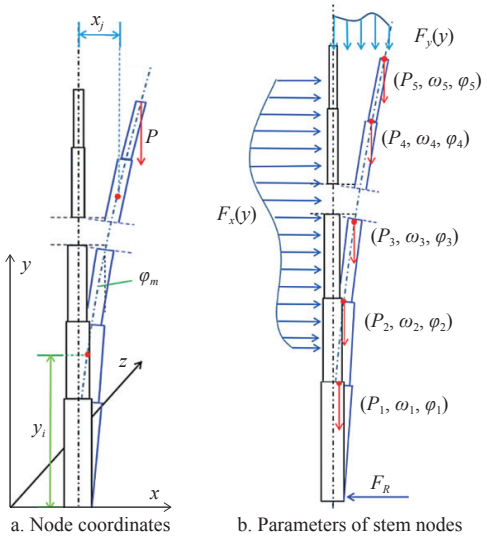


a. Node coordinates b. Parameters of stem nodes

Figure 4 Mechanical model of rice stem

When modeling, considering that the dead weight of the rice ear will generate a bending force, resulting in a complete constraint, and the upper end is free, the bending-deflection curve equation of rice stem under the influence of rice ear is established, and the deflection and node turning angle of each stage of the stem are solved. Naturally, under the condition of no external load, the rice stem is only affected by the weight of the ear, so the approximate differential equation of the deflection curve can be established[37], as

follows:

$$\frac{\mathrm{d}^2\omega}{\mathrm{d}y^2}=\frac{M(y)}{EI} \tag{5}$$

$$M(y)=-[P(x_0-x)]+F_{\cos\varphi_m}(x_m-x)F_{\sin\varphi_m}(y_m-y) \tag{6}$$

where, $\omega$ is the deflection of the rice stem, m; $y$ is the vertical distance from the measurement point to the ground, m; $x$ is the horizontal distance from the measurement point to the neutral axis, m; ($x_m$, $y_m$) is the coordinates of the measurement point, is rotation angle of measuring point; $M$ is the bending moment of the stem, N·m; $EI$ is the rice section stiffness, N·m$^2$; The moment of inertia of the thin-walled ring is $\pi R^3\delta$; $P$ is the rice weight, N; $F$ is free load, N. Due to the large deformation of the stem, this study introduced the Simpson equation[38] to characterize and solve the deflection, as follows:

$$\frac{\mathrm{d}^2\omega}{\mathrm{d}y^2}=\frac{M(y)}{EI}\left\{1+\left(\frac{\mathrm{d}\omega}{\mathrm{d}y}\right)^2\right\}^{1.5} \tag{7}$$

By integrating Equation (7), the stem deflection curve and the differential equation of the turning angle can be obtained, since the Equation (7) involves nonlinear implicit elliptic integrals, this paper introduces the fourth-order Runge-Kutta method[39] for numerical calculation, as follows:

$$\begin{cases}\dfrac{\mathrm{d}\omega}{\mathrm{d}y}=f(y,\omega)\\ \left.\dfrac{\mathrm{d}\omega}{\mathrm{d}y}\right|_{y=0}=0\end{cases} \tag{8}$$

The Runge-Kutta method is an important class of implicit or explicit iterative methods for the solution of nonlinear ordinary differential equations. The solution algorithm is shown in Equation (9), where $h$ is the calculation step size.

$$\begin{cases}\omega_{i+1}=\omega_i+\dfrac{1}{6}(k_1+2k_2+3k_3+k_4)\\ k_1=\mathrm{hf}(y_n,\omega_n)\\ k_2=\mathrm{hf}\left(y_n+\dfrac{h}{2},\omega_n+\dfrac{k_1}{2}\right)\\ k_3=\mathrm{hf}\left(y_n+\dfrac{h}{2},\omega_n+\dfrac{k_2}{2}\right)\\ k_4=\mathrm{hf}(y_n+h,\omega_n+k_3)\end{cases} \tag{9}$$

From Equation (6)-(9), the initial solution of the deflection curve equation can be obtained. It can be seen that the deflection of rice stem is related to Young's modulus and section stiffness. Therefore, the stiffness is first solved by combining the geometric relationship. Under the influence of the comprehensive load, the deformation of the stem is simplified as shown in the figure, and the Equation (7) can be deformed as:

$$\frac{\mathrm{d}^2\omega}{\mathrm{d}y^2}\left\{1+\left(\frac{\mathrm{d}\omega}{\mathrm{d}y}\right)^2\right\}^{1.5}=\frac{\mathrm{d}\varphi_m}{\mathrm{d}y}\cos\varphi_m \tag{10}$$

Integrate Equation (10) to get its basic solution. On this basis, this study is extended to solve the applied load of rice, as shown in Figure 5. The natural load is decomposed into horizontal and vertical forces, and the rice gravity is simplified to the center of gravity.

The deformation model of the stem axis in Figure 5 can describe the bending and micro-deformation degree of the stem under load, and can be described by the angle of rotation and the amount of axial deformation. From the geometric relationship in Figure 5, it can be seen that:

$$\phi_m=\arctan\left(\frac{y_m}{x_m}\right)=2\tan^{-1}\left(\frac{y_m}{x_m}\right) \tag{11}$$

$$\frac{\mathrm{d}l}{\mathrm{d}s}=\cos(\varphi_m-\varphi)=\frac{\mathrm{d}\varphi}{\mathrm{d}s}\frac{\mathrm{d}l}{\mathrm{d}\varphi}=\frac{M}{EI}=\frac{\mathrm{d}l}{\mathrm{d}\varphi} \tag{12}$$

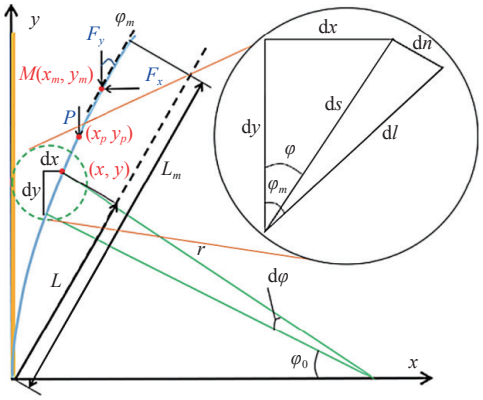


Figure 5 Loading and deformation of rice

Therefore, taking Equation (12) into Equation (10), it can be obtained that the ground end of the stem is completely constrained, so the bending angle can be expressed as:

$$\cos\varphi_m=\frac{M}{EI}\frac{\mathrm{d}l}{\mathrm{d}s}r \tag{13}$$

$$r=\sqrt{1+\omega'^2} \tag{14}$$

where, $r$ is the radius of curvature of the segment, mm. Equations (7)-(14) and (2) can be solved to obtain the deflection curve equation of the stem under load, but it noticed that the stiffness of the stem is still necessary. Therefore, this study used the deflection to determine the stiffness of the stem. The solution is to describe the stiffness of the stem at different positions with the change of displacement.

Stem ground end, d$l$≈d$s$, $\omega$≈0, And the bending angle of the proximal end is 0, therefore, Equation (13) can be transformed into:

$$\cos\varphi_m=\frac{M}{EI}\sqrt{1+\omega'^2} \tag{15}$$

The bending stiffness of the stem at this time can be solved as:

$$EI=\frac{M(0)}{\sqrt{1+\omega'^2_m}} \tag{16}$$

For general parts, Equation (7) can be transformed into:

$$\cos\varphi\frac{\mathrm{d}\varphi}{\mathrm{d}y}=-\frac{M(y)}{EI} \tag{17}$$

Substituting Equation (6) into Equation (17), and integrating both sides of the equation, Equation (18) can be get:

$$\sin\varphi=-\frac{[P(x_0-x)+F\cos\varphi_m(x_m-x)]}{EI}-\frac{[F\sin\varphi_m(y_m-y)]^2}{2EI} \tag{18}$$

Therefore, this paper calculated the stiffness value of each internode based on the deformation deflection and rotation angle of the stem from the Equation (18). After obtaining the calculation method of the stiffness of the stem, the critical load of the rice stem and the position of the internodes that are prone to failure are further discussed. Since the lodging form of the stem is mainly bending failure, Brazier[40] is used to calculate the critical bending load of the stem, predict the lodging load of the rice stem and determine the approximate lodging interval. The stem model in this

study is a thin-walled ring, so the critical load in Brazier's theoretical model is:

$$M_{cr} = 0.314\,26\frac{\pi E\delta^2 R}{(1-\nu^2)^{\frac{1}{2}}} \tag{19}$$

where, $\nu$ is the Poisson's ratio of the stem, which is taken as 0.3 in this study[28]. From Equation (20), it can be known that the critical bending load of each joint can be solved by combining parameters such as moment of inertia and radius after the stiffness is solved. Combined with Equations (19) and (20), the critical load of each segment can be solved based on the deformation.

### 2.4 Bending mechanics tests based on stem loading model at room temperature

In order to reveal the mechanical properties of stems at different temperatures, this study firstly designed a cantilever bending mechanical property test of stems at room temperature. In order to ensure the accuracy and consistency of the test temperature, the selected rice plants were preliminarily screened and grouped according to their different parts and differences in width and thickness. A digital microwave incubator is used for sample temperature heating and heat preservation. The schematic diagram of the test structure and the test process are shown in Figure 6. At the same time, the test samples including stems, leaves, roots and other parts were heated and kept warm under a digital incubator. The MM721NG1-PW digital microwave thermostat selected in this test can quickly and accurately reach the specified temperature. The temperature is controlled by an infrared thermometer during the test. The measurement temperature range is –18°C to 35°C, and the measurement accuracy is 1.8%.

In this study, the samples were subjected to the cantilever bending test under normal temperature treatment and the three-point bending test under normal temperature treatment on the Edberg 0824 push-pull testing machine to analyze the bending deformation under load of the stem at different temperatures - the axial and radial directions at the time of fracture. The change characteristics of stiffness to reveal the bending resistance mechanism of stems at different temperatures, and provide theoretical guidance for the mechanized harvesting of mature rice.

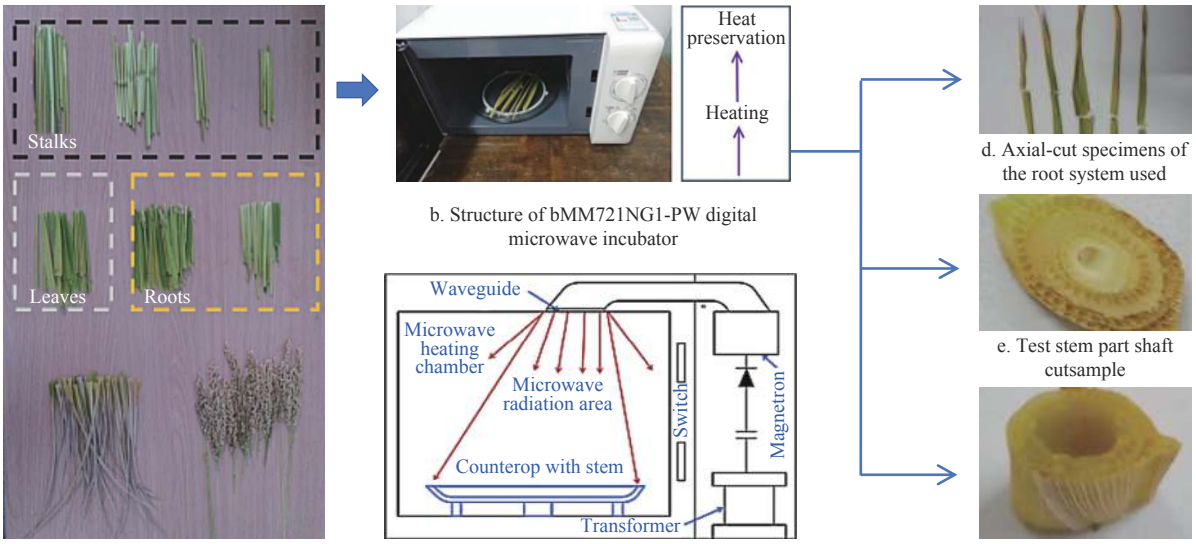


a. Grouping of rice samples

b. Structure of bMM721NG1-PW digital microwave incubator

c. Principle and heating process of digital incubator

d. Axial-cut specimens of the root system used

e. Test stem part shaft cutsample

f. Root system shaft cut sample used in the experiment

Figure 6 Cutting of rice stem samples

When rice lodging occurs, each segment of the stem, especially the proximal segment, is subject to bending stress under the combined effect of ear weight and external load. That is, one end is fixed and the other end is free, which can be regarded as a cantilever beam model. The purpose of this test is to verify the bending resistance of rice stems, set up a single-arm bending test of No. 3 stems at room temperature, and analyzed the bending resistance of rice stems. The experimental design and sample installation are shown in Figure 7.

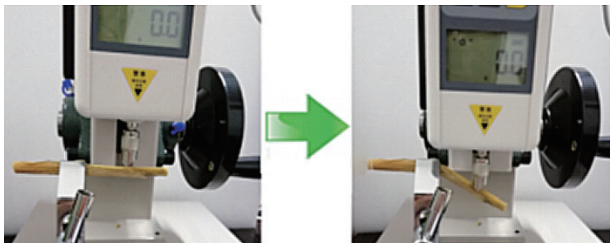

Figure 7 Installation method for single-arm bending test

Put the three groups of test samples into the incubator for temperature adjustment, and adjust the test temperature to 20°C, in order to reduce the influence of the indoor temperature difference on the test, after the value of the incubator remains unchanged, it is taken out for about 1 h. In order to ensure the accuracy of the test results, the stems were kept in a relaxed state when clamping to avoid substantial damage to the stems themselves.

Similarly, before the three-point bending test, the rice stem samples were grouped, and the three-point test method was carried out for each part to measure the bending resistance, and the main section of its lodging was observed, mainly the No.3 near the lot. The force state of the three parts of the stalk during the test is shown in Figure 8.

The measurement principle of the three-point method is to fix the two ends of the test material, apply a load in the middle, and measure the characteristics of the crop based on the bending theory of the beam. When the rice is lodging, most of the cases on the upper end of the stem can be regarded as the plastic deformation of the stem caused by the excessive load in the middle of the internode, which can be approximated as a three-point stress treatment. Figures 8a-8c correspond to the experimental procedure at the root, middle and top of the stalk, respectively. All data were saved for subsequent processing and analysis at the end of the test.

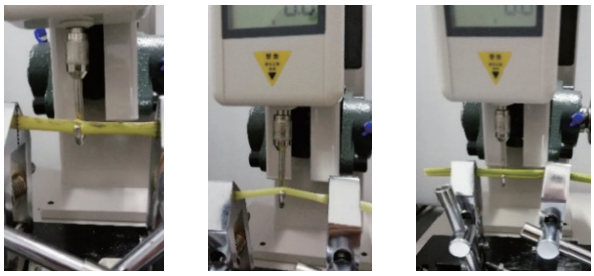

a. stem root b. middle stalks c. top of stalks

Figure 8 Three-point tension mounting of the blade

### 2.5 Bending test of stem under temperature difference induced stress

The main purpose of this part is to study and analyze the mechanical properties of rice stems under the simulated natural environment of day and night temperature changes. Before the experiment, the experimental materials were screened, and the samples were placed in the refrigerator for 24 h before classification, and kept in the incubator for heat preservation, so as to basically ensure that the physical properties of each segment tend to be consistent. During the test, the stems were first treated with temperature difference, and the tensile properties of the leaves at different temperatures were tested and analyzed using the existing test materials.

In order to achieve the change of temperature difference between day and night, the mechanical properties of rice leaves in the range of −10°C to 65°C were studied. The specific temperature test equipment and control method are shown in Figure 9.

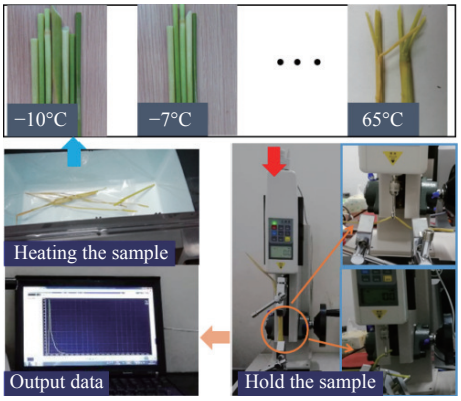


Figure 9 Broken force test of stem at different temperatures

They were grouped according to their internode positions, and divided into the third stem at the proximal end. The stem samples were placed in a digital microwave incubator and microwaved for 8 min. After the rice stems had completed the temperature treatment, the samples were clamped and immediately subjected to the second stage of the three-point stretching test. The fixture used for stretching was mounted and calibrated on the test apparatus, connected to an Eidelberg 0824 push-pull tester with a computer and the three-point stretching test was carried out until the stems broke, the load data was exported and the fractures were analyzed. The temperature was increased by 3°C each time. The test temperatures are −10°C, −7°C, 0°C, ..., 65°C, respectively.

## 3 Results and discussion

### 3.1 Vascular bundle distribution gradient and regression model

Under the electron microscope, the microstructure morphology and fibrous tissue arrangement of roots and stems of different plants are basically the same, as shown in Figure 10. Rice stems are characterized by a well-defined layered structure with thin walls and tube bundles evenly arranged, and the microscopic composition is a solid cylindrical structure with multiple laterally reinforced nodes; the root cells are arranged neatly, clearly and compactly, from small to large from the inside to the outside. In the form of radial arrangement, the parenchyma cells of the cortex are the smallest and the density is high, and the cells of the outer cortex are neatly arranged and evenly distributed.

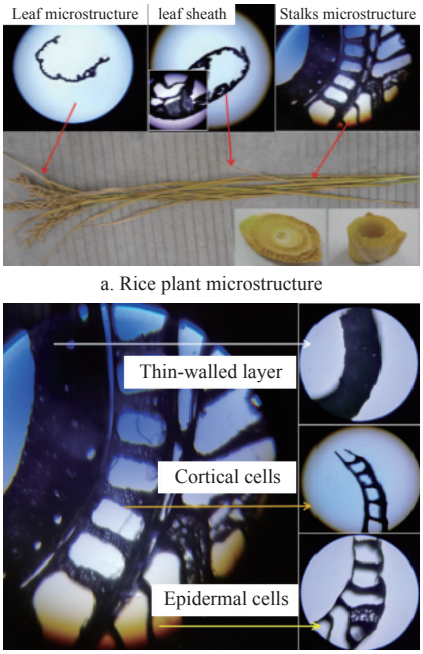


a. Rice plant microstructure

b. Stem microstructure and arrangement

Figure 10 Microstructure of rice plants and stems

In addition, under the microscope, the volume content of vascular bundles showed a decreasing trend from bottom to top, and the vascular bundles near the epidermis are denser than those in the core, the density and existence of vascular bundles and epidermal mechanical tissue layers are important factors that determine the mechanical properties of rice. Therefore, it can be preliminarily inferred that there is a certain difference in the stiffness of the vascular bundle in the axial and radial directions.

In this study, the hue adjustment and grayscale processing were performed on the stem microstructure in Adobe illustrator, and the RGB was set to (0, 0, 0) based on MATLAB, that is, the black mark is the vascular bundle, and its area ratio was calculated, for each group of 5 samples, the proportion of the vascular bundle area in the first, third, fifth, and seventh internodes was counted, as shown in Figure 11.

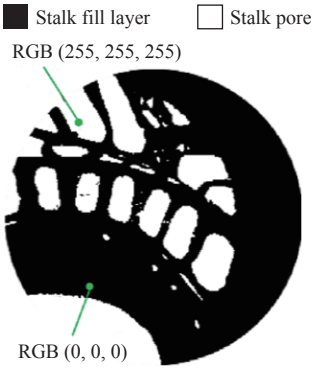


Figure 11 Vascular bundle labeling and area ratio extraction

In order to reveal the relationship between the content of stem vascular bundles and their location, this study obtained a significant relationship between the proportion of stem vascular bundle area and its location through one-way analysis of variance. As listed in Table 1. The results showed that there were extremely significant differences in the area of stem vascular bundles among the four groups, indicating that the content of vascular bundles was significantly correlated with the position of stems.

**Table 1 One-way analysis of variance for the proportion of stem vascular bundles in the four groups**

| Variation | df | SS | $s^2$ | $F$ | $F_{0.05}$ | $F_{0.01}$ |
|---|---|---|---|---|---|---|
| Between blocks | 3 | 0.2744 | 0.0914 | 77.82* | 3.24 | 5.29 |
| Within the block | 16 | 0.0188 | 0.0018 | | | |
| Total variation | 19 | 0.2932 | | | | |

In this study, the exponential regression model of vascular bundle content and internode position was further established, and the relationship between vascular bundle content and internode position in stems was obtained as follows:

$$\Lambda = 0.9774e^{-0.005\,368\pi} \tag{20}$$

where, $\Lambda$ indicates vascular bundle content. The model regression root mean square error (RMSE) was 0.0734, the coefficient of determination ($R^2$) was 0.8073, and the modified coefficient of determination ($R^2_{Adj}$) was 0.7055, which showed that the regression equation was in good agreement with the test values as a whole.

The comparison between the experimental results and model predictions of internode location and vascular bundle content is shown in Figure 12. The error between the test results and the model prediction results is small, and the prediction model can better reflect the test results and laws.

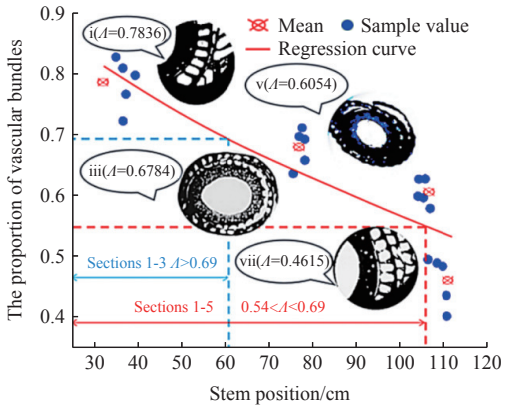


Figure 12 Microstructure of stems of different plants

It can be seen from Figure 12 that the content of vascular bundles in the stem gradually decreased, and the vascular bundles are an important component to maintain the mechanical properties of the stem. Therefore, it can be preliminarily predicted that the mechanical properties of the stem gradually decrease from bottom to top, the 1st to 3rd joints have the largest bending moment and the best mechanical properties, the 4th to 5th joints are the second, and the 6th to 7th joints have the worst bending performance. This study establishes a variable stiffness mechanical model of the stem to reveal the maximum load-bearing position of the stem.

### 3.2 Prediction of culm stiffness and easy lodging position of each segment

After completing the establishment of the variable stiffness mechanical model of the stem, this study preliminarily predicted the stiffness of different parts of the stem based on the mechanical model, and determined the stiffness distribution of each segment of the stem.

In the calculation, the load acting point was fixed on the top of the stem, and the ear weight of Huaidao No.10 was 0.42 N, which acted on the end of the stem, and the direction was vertical downward; the load of the test sample was controlled using a 139 digital force gauge (model: ZP-10, capacity: 10 N, resolution: 0.001 N, Dongguan Fuma Electronic Equipment Co., Ltd., China), a lateral force of –0.5-0.5 N is applied to the rice, the direction is horizontal, and the loading interval is 0.2 N. After measuring the end corner and each segment corner, the corresponding stiffness value can be obtained. The test environment is 25°C. In this study, the critical bending moment is converted into a critical load force by combining the strength equation of bending moment and stress in material mechanics, and the torsional section coefficient is:

$$W_{\text{ti}} = \frac{\pi d_i^3}{16}\left(1-\alpha_i^4\right) \tag{21}$$

where, $\alpha_i = \delta/d_i$, in this paper, only the bending deformation is carried out, and the torsional deformation of the stem is ignored, and the bending moment can be further transformed into the load acting on the stem. The load is applied to the middle of the stem, and the bending section coefficient is:

$$W_{zi} = \frac{\pi d_i^4}{32}\left(1-\alpha^4\right) \tag{22}$$

$$F = \frac{M_i}{W_{zi}}\frac{\pi d_i^2}{4} \tag{23}$$

Combined with Equations (18)-(23), the elastic modulus and flexural stiffness of each segment of the stem were calculated in this study, and the mechanical properties of each segment of the stem were obtained as shown in the figure below.

The predicted results are shown in Figure 13. It can be seen from Figure 13a that in the prediction model of stem stiffness, the stiffness value of the No. 3 stem is the largest was 2.39 GPa, which indicated that the mechanical properties of mature stems mainly depended on the 1-3 internodes. Figure 13b shows the relationship between the flexural stiffness of the stem and its position. It can be seen that the flexural stiffness of the stem in the 5-7 internodes is very small and cannot be used as a support carrier for the stem; stem No.1 had the highest bending stiffness and was the main bearing structure of the culm. Further, an exponential regression model was established for the flexural stiffness of the stem at different positions, and the relationship between the flexural stiffness of the stem and the position of the internodes was obtained as follows:

$$\rho = 0.6182e^{-0.3694\pi} \tag{24}$$

The model regression root mean square error (RMSE) was 0.022 52, the coefficient of determination ($R^2$) was 0.9859, and the modified coefficient of determination ($R^2_{Adj}$) was 0.9789. Based on the calculation of the anti-bending stiffness, the maximum load of each segment of the stem is calculated with the help of Equations (19)-(23), as shown in Figure 14.

The stress-bending moment diagram of No.3 stem under the action of comprehensive load is shown in Figure 15a, the dangerous section, is the axial section of the load concentration point, where the shear force-bending moment mutation also occurs. In these two places, the two sides of the neutral axis of the stem are tensile stress and compressive stress, respectively. Calculated as follows:

$$\sigma_{c\max} = \sigma_{t\max} = \frac{M_4^* d_3}{2I_z} \tag{25}$$

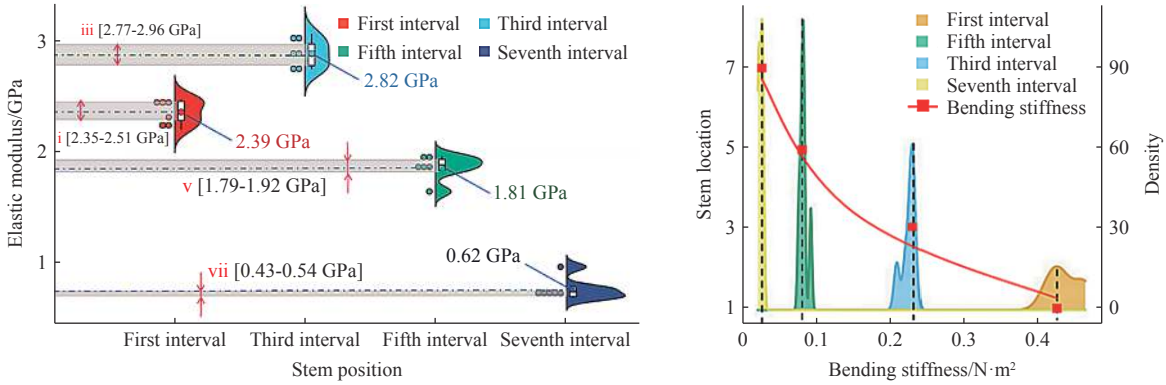


a. Statistical distribution of elastic modulus b. Statistics and regression model of stem bending stiffness

Figure 13 Prediction of mechanical properties of stem based on mechanical model

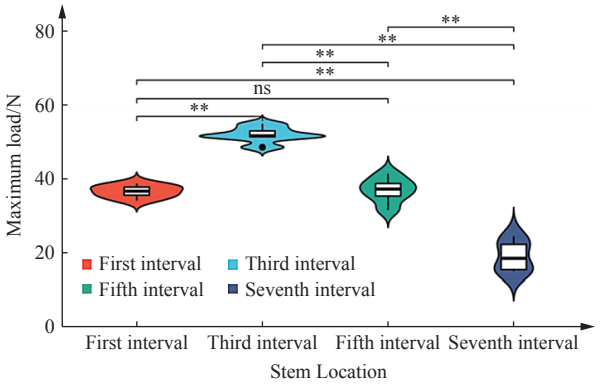


Figure 14 Prediction and loading of internode load of stem

where, $M_4^*$ is the interaction bending moment between the No.4 stem and No.3 stem, N·m; $\sigma_{c\max}$ is the maximum compressive stress, GPa; $\sigma_{t\max}$ is the maximum tensile stress, GPa.

Conclusion can be made, the force concentration point of No.3 stem is the main lodging point of Huaidao No.10, the maximum stress is located at the boundary point of the section, and the stress is linearly related to the radius from the center of the section.

### 3.3 Rice stem bending test at room temperature

In this study, the two-point bending test of rice stems was firstly carried out at room temperature to determine the bending resistance of rice stems. After the experiment was repeated three times, the experimental data was exported. The experimental results are shown in Figure16.

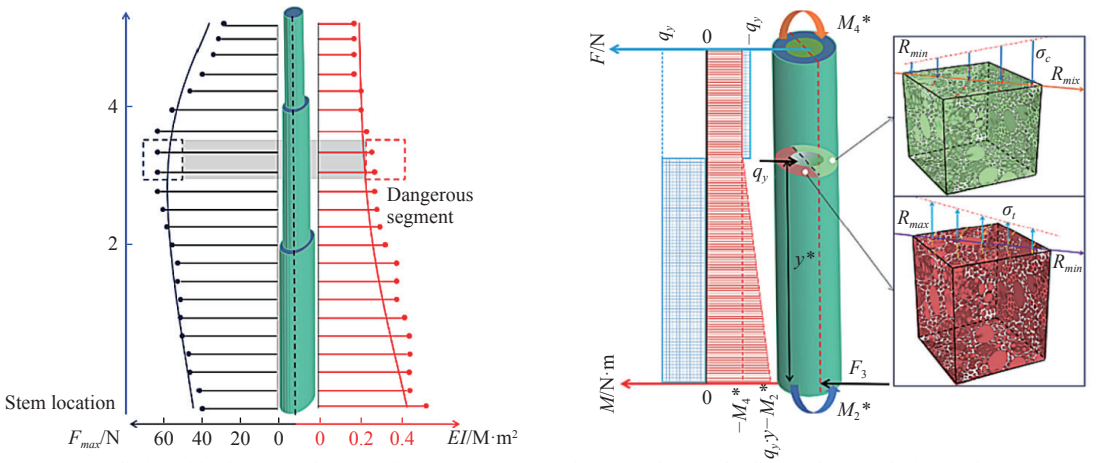


a. Prediction of loading on each part of the stem b. Comprehensive loading analysis on the internodes of stem No.3

Figure 15 Comprehensive prediction of stem loading based on variable stiffness mechanical model

It can be seen from the experimental results that the maximum bending force of rice stem samples A, B, and C is significantly different. For sample C, the maximum bending force can reach 1.32 N. In contrast, the maximum bending force of samples A and B is only 0.2-0.4 N. This may be due to the large internode dry weight and dry matter mass of sample C, which significantly improved the bending resistance of rice stems. In addition, the relationship between internode length and bending resistance was not significant.

In order to explore the deformation of rice stems under lateral loading, a three-point bending test was designed. The analysis of the exported test data is shown in Figure 17. It can be seen that during the deformation process of the stem, the force changes obviously and there are two obvious peaks. The first peak occurred earlier, and

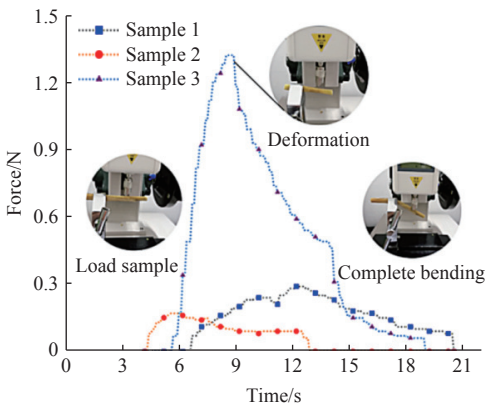


Figure 16 Results of two-point bending test of rice stem

when the tensile force was 5-13 N, the first peaks were generated for samples 1 to 3; at the second peak, the stem was completely destroyed and pulled off. It can be obtained that the stem lodging occurs at the first peak. The ultimate tensile force of the stem of sample No.1 is 23.6 N, compared with that of sample No.3, which is only 12.6 N.

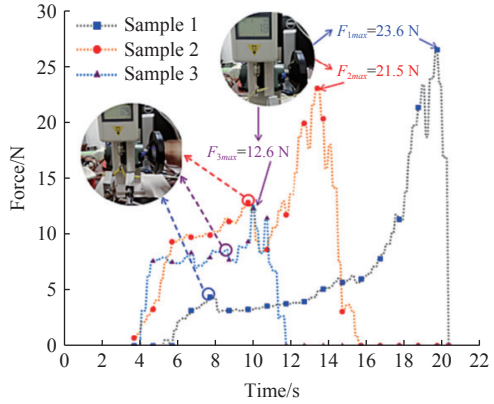


Figure 17 Three-point bending test of rice stem at room temperature

After the first peak of the stem loading, the stem pulling force will continue to rise, which is due to the bending of the axial vascular bundles, so that the rice stems can still be connected, the deformation force of rice is transformed from bending force to axial tissue connection force. The homogeneity of the axial performance of the rice stem determines that it has good mechanical properties in the axial direction, so the tensile fracture force is larger.

In summary, the mechanical properties of rice stems in the radial and axial directions are significantly different. During the three-point lateral loading test, the deformation of rice can be divided into two stages. When the lateral load of the stem is greater than the maximum force in the first stage, the rice will lodging; in the second stage, the deformation mode of the stem is tensile deformation. When the axial tension limit of the stem is reached, the rice stem is completely destroyed. The gradient distribution of vascular bundles in rice stems makes them show high modulus and low toughness when they are laterally flexed, thus showing low-level bending failure and high-level fracture failure.

### 3.4 Rice stem tensile under the temperature difference

Based on the previous experimental data, the three-point bending curves of rice stalks at –10°C to 4°C as shown in Figure 18 were generated in Origin software. It can be seen that the ultimate tensile force of the stem under the two temperature treatments of –10°C and –7°C was significantly higher than that of the other five groups. At 10°C, the ultimate tensile force of the stem was 3.8 N, and at –7°C, the ultimate tensile force could reach 6.1 N, and then with the increase of temperature, the ultimate tensile force of the stem was less than 0.5 N. This indicates that at low temperature, the stem is prone to bending deformation. At the same time, under the 7 treatments, there was no two-stage destruction of rice culm, indicating that low temperature treatment has a negative impact on the morphological distribution of vascular bundles and the establishment of functional gradients.

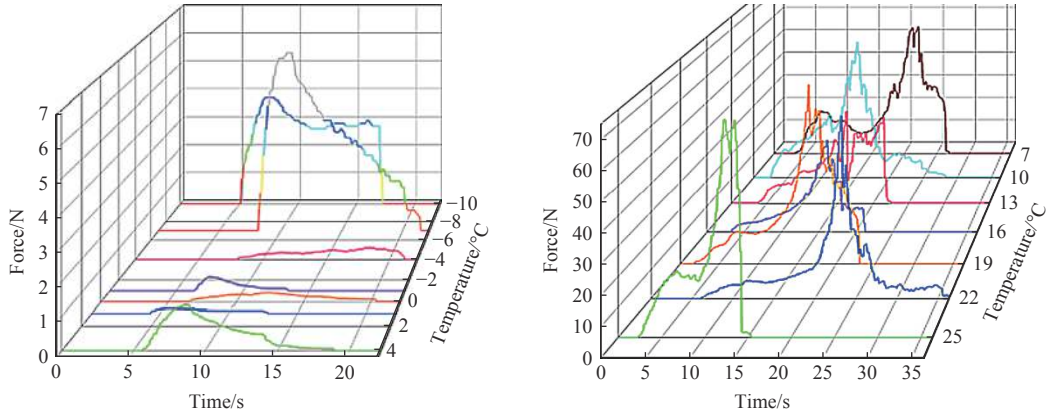


a. Three-point bending test of rice stem at −10°C-4°C b. Three-point bending test of rice stem at 7°C-25°C

Figure 18 Three-point bending test of rice stem at –10°C-25°C.

Under the treatment of 7°C-25°C, the ultimate tensile force of rice stem is shown in Figure 18b. Under this temperature treatment, the ultimate tensile force of rice increased significantly. Under the 7 groups of temperature treatments, the ultimate tensile force of the stem was all greater than 50 N. At the same time, under the treatment in this group, the bending deformation regularity of rice stems was obvious, showing obvious periodic bending-breaking stages. It can be considered that when the lateral load reaches a certain value, the stem will bend and convert the radial load into the axial load. Under the action of the gradient functional arrangement of the vascular bundle, the axial display of the stem is higher. The axial stiffness protects the rice from being completely damaged.

Under the treatment of 28°C-46°C, the ultimate tensile force of rice stem is shown in Figure 19a. Under this group of temperature treatments, the ultimate tensile force of rice further increased, reaching 88 N at 43°C, and then decreasing, reaching 57.3 N at 46°C. At the same time, within 10 s before loading, a slow bending stage is still presented, as shown in Figure 19b. When the temperature is 34°C, the lodging force reaches 38.3 N. After the temperature was 37°C, the lodging point of rice stem disappeared, the possible reason is that under high temperature treatment, the dissipation of dry matter stored in rice stems is accelerated, and the distribution of vascular bundles is destroyed, thereby affecting the lodging resistance of rice.

Under the treatment of 49°C-65°C, the ultimate tensile force of rice stem is shown in Figure 20, in this group of temperature difference treatments, the ultimate tensile force of rice stems decreased again, this indicates that too high temperature will no longer be suitable for the growth and development of rice, and will have a serious impact not only on yield but also on the mechanical properties of rice.

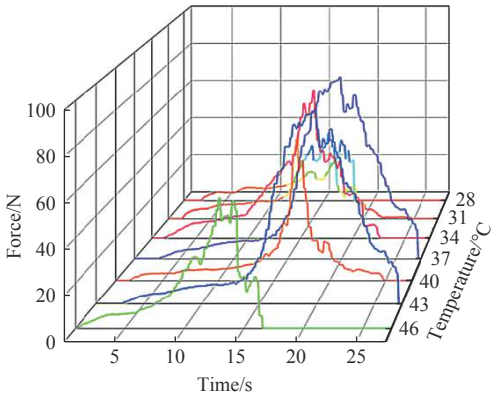


a. Three-point bending test of rice stem at 28°C-46°C

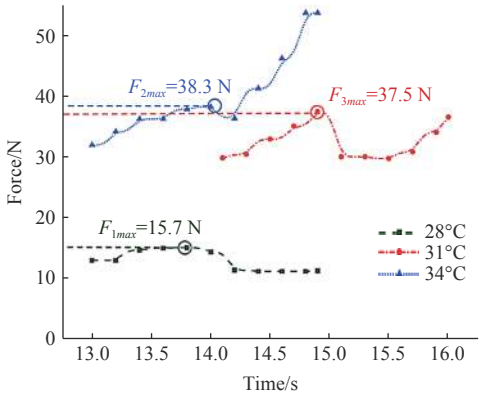


b. Lodging force of rice stem at 28°C-34°C

Figure 19 Three-point bending test of rice stem at 28°C-65°C

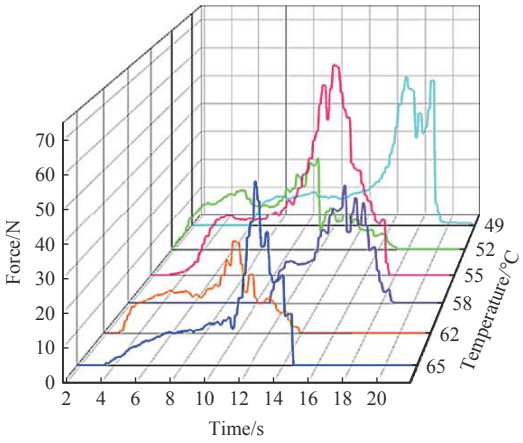


Figure 20 Three-point bending test of rice stem at 49°C-65°C

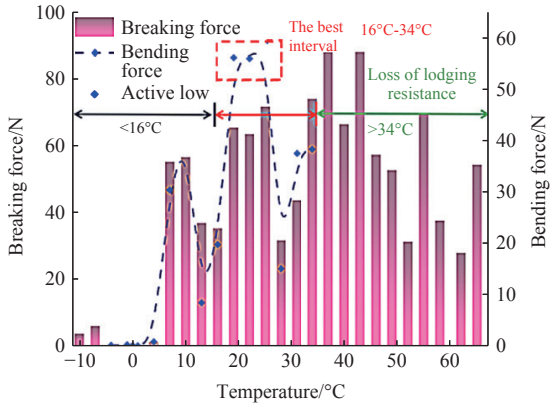


Figure 21 Analysis of ultimate tensile force and lodging force of rice stem in three-point bending test

The distribution law of ultimate tensile force and lodging force of No.3 stem under each temperature treatment was calculated, as shown in Figure 21. From the fitting curve of lodging resistance, it can be seen that the optimal cultivation temperature of Huaidao 10 at the maturity stage is about 16°C to 34°C. In this temperature range, the lodging force of rice is above 80 N, indicating that the vascular bundle of rice grows well at this temperature, thus maintaining the mechanical properties of rice well.

In this study, further three-point bending mechanical tests were carried out on the No.1-4 stems at 16°C-34°C, and the interval group was set at 0.2°C. The mechanical model established above and the predicted value of ultimate tensile force were verified, and the bending-lodging-fracture process of rice stem at this temperature was analyzed and statistically tested, as shown in Figure 22. It can be seen from Figure 22 that the deviation of the No.3 stem prediction model is small. In the *t*-test, with a

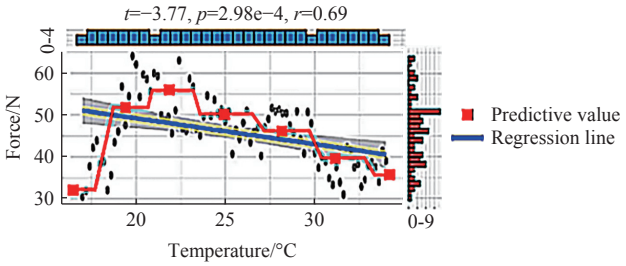


a. Statistical test of bending force of No. 1 stem

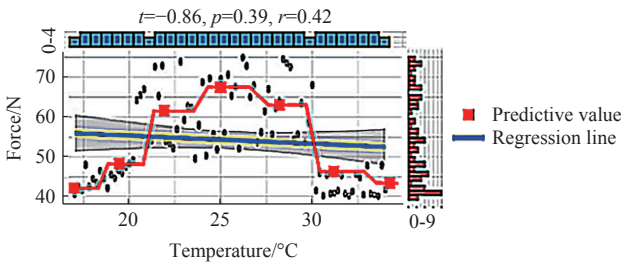


b. Statistical test of bending force of No. 2 stem

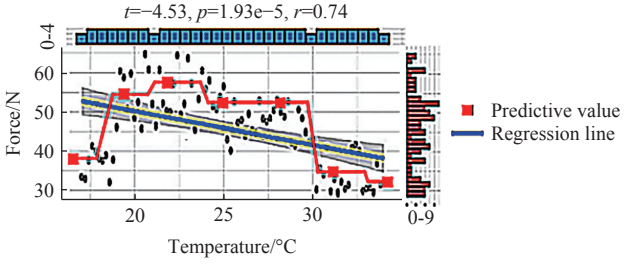


c. Statistical test of bending force of stem No.3

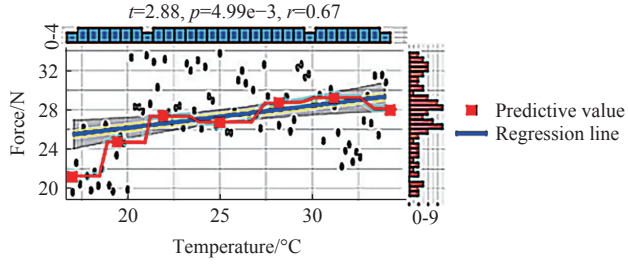


d. Statistical test of bending force of stem No.4

Figure 22 Statistics and *t*-test of the bending force of No.1-4 stems at 16°C-34°C

$p$-value≪0.05, the results were not statistically significantly different and could be a better predictor of the magnitude of the inversion force based on the deformation of the stem.

In order to provide the physicochemical index of the bending force of the stem under different temperature difference treatments, this paper established the bending force correction coefficient TF of the No.3 stem at different temperatures. As shown in Equation (25), after temperature correction, the lodging force of mature rice in natural state can be predicted according to Equations (6) and (21)-(24). As shown in Equation (26), the lodging force calculation equation of field mature rice based on the variable stiffness mechanical model at different temperatures is obtained.

$$T_F = 0.9551\exp\frac{-(T-28.85)^2}{9.917} \tag{26}$$

$$F_B = T_{F'}\frac{M_4^* d_3}{2I_z}\frac{\pi d_3^2}{4} \tag{27}$$

where, $F_B$ is the lodging force, N. Taking Huaidao No.10 as an example, this paper conducts statistical analysis on mature Huaidao, rice matures from July to August. During this period, the peak sunshine time is 3.1-3.8 h a month. The temperature is relatively high, and the maximum temperature can reach 32°C. In this study, the temperature in Huai'an area was detected, and the safe growth area and lodging danger area of stems in one day were calculated as shown in Figure 23.

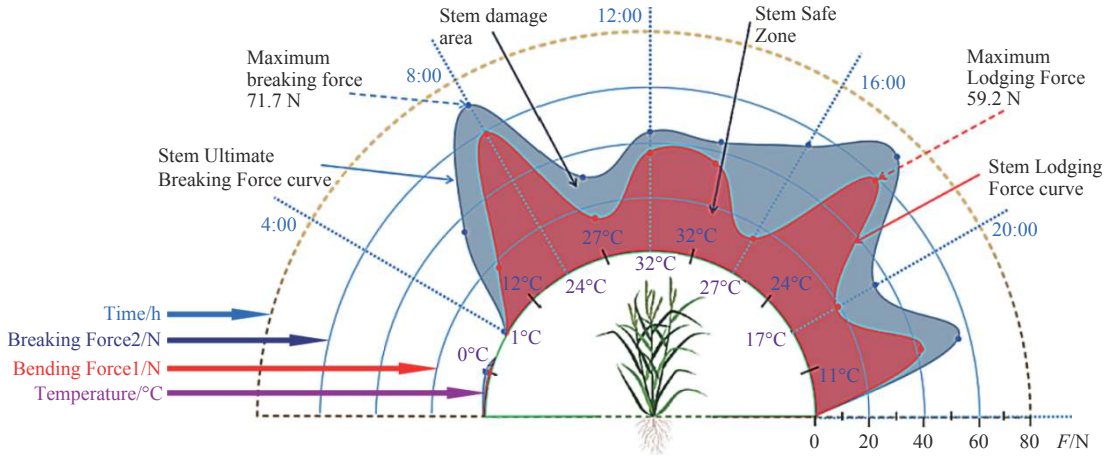


Figure 23 Sunshine time and mechanical properties of rice stems in Jiangsu, China

It can be seen from Figure 23 that the heat accumulation in Huai'an area is larger, and the mechanical properties of the stem are better. Between 8:00 and 16:00, the safe growth area of the stem is larger. But within the peak sunshine range, the danger zone expands. The machine harvesting time of rice should be avoided as much as possible.

## 4 Conclusions

1) In this study, a microstructure observation experiment was carried out for Huai Rice No.5 variety, extracted statistics on the area share of different parts of stalks based on MATLAB, and established a bottom-up exponential regression model for the share of vascular bundles of stalks, and found that the vascular bundles in the 1st-3rd internodes were above 69%, and the vascular bundles in the 4th-5th internodes were above 54%, with an RMSE of 0.0734, and an $R_{\mathrm{Adj}}^2$ of 0.7055, which was a good fit. The results showed that the microstructure of the stalks had an obvious gradient arrangement law, and its mechanical properties varied linearly from bottom to top.

2) A free load was applied to the mature rice stem in its natural state, and the stiffness value of the stem was determined by measuring the deflection or turning angle. It was found that the load on the third stem was the highest, approximately 52.68 N, significantly different from the loads on other internodes. This indicates that based on the measurement results of the static parameters of the stem and applied to a case of a free load to the mature rice stem in the natural state, the stiffness value of the stem was obtained by measuring the deflection or turning angle of the stem. Using this model, the lodging force of the third internode at a temperature of 25°C was predicted. It was found that the load on the third stem was the largest, about 52.68 N, significantly different from the load on other internodes. This indicates that the third internode is likely to be the main lodging point of the rice plant.

3) Furthermore, to identify the temperature range in which the third internode is prone to bending, two-point bending test and three-point bending test under a temperature ranged from –10°C to 65°C. In the three-point bending test, the stress on the stem of rice exhibited two distinct stages. It was concluded that the stem had high toughness and low modulus in the lateral direction, while high modulus and low toughness in the axial direction. Additionally, the bending force correction coefficient was established. The optimum temperature range for lodging resistance of the stem was determined to be between 16°C and 34°C. This finding is crucial in ensuring the mechanical harvest of rice.

## Acknowledgements

This research work was supported by the National Natural Science Foundation of China (Grant No. 52175235), Natural Science Foundation of Jiangsu Province (Grant No. BK20221368), Key Laboratory of Modern Agricultural Equipment and Technology (Jiangsu University), Ministry of Education (Grant No. MAET202326), and Project Funded by the Priority Academic Program Development of Jiangsu Higher Education Institutions (Grant No. PAPD-2023-87).

## [References]

[1] Tang Z, Liang Y Q, Wang M L, Zhang H, Wang X Z. Effect of mechanical properties of rice stem and its fiber on the strength of straw rope. Industrial Crops & Products, 2022; 180: 114729.

[2] Zhang T, Li Y M, Xu L Z, Liu Y B, Ji K Z, Jiang S. Experimental study on fluidization behaviors of wet rice threshed materials with hot airflow. Agriculture, 2022; 12(5): 601.

[3] Ministry of Agriculture and Rural Affairs of China. Annual Rice

Production in China. 2020. https://data.stats.gov.cn/ easyquery.htm?cn= C01 Accessed on [2021-04-05]. (in Chinese)
[4] Liu Y B, Li Y M, Chen L P, Zhang T, Liang Z W, Huang M S, et al. Study on performance of concentric threshing device with multi-threshing gaps for rice combines. Agriculture, 2021; 11(10): 1000.
[5] Liu W J, Luo X W, Zeng S, Zang Y, Wen Z Q, Zeng L, et al. Numerical simulation and experiment of grain motion in the conveying system of ratooning rice harvesting machine. Int J Agric & Biol Eng, 2022; 15(4): 103–115.
[6] Li B, Du X, Fei Y Y, Wang F Q, Xu Y, Li X. Efficient breeding of early-maturing rice cultivar by editing PHYC via CRISPR/Cas9. Rice, 2021; 14: 1–4.
[7] Khir R, Atungulu G, Chao D, Pan Z L. Influence of harvester and weather conditions on field loss and milling quality of rough rice. Int J Agric & Biol Eng, 2017; 10(4): 216–223.
[8] Zhuang X B, Li Y M. Segmentation and Angle Calculation of Rice Lodging during Harvesting by a Combine Harvester. Agriculture, 2023; 13(7): 1425.
[9] Tang Z, Zhang B, Wang M L, Zhang H T. Damping behaviour of a prestressed composite beam designed for the thresher of a combine harvester. Biosystems Engineering, 2021; 204: 130–146.
[10] Liu Q H, Ma J Q, Zhao Q L, Zhou X B. Physical traits related to rice lodging resistance under different simplified cultivation methods. Agronomy Journal, 2018; 110(1): 127–132.
[11] Liang Z W, Wada M E. Development of cleaning systems for combine harvesters: A review. Biosystems Engineering, 2023; 236: 79–102.
[12] Hong W Y, Chen Y J, Huang S H, Li Y Z, Wang Z M, Tang X R. Optimization of nitrogen-silicon (N-Si) fertilization for grain yield and lodging resistance of early-season indica fragrant rice under different planting methods. European Journal of Agronomy, 2022; 136: 126508.
[13] Ding B C, Liang Z W, Qi Y Q, Ye Z K, Zhou J H. Improving cleaning performance of rice combine harvesters by DEM-CFD Coupling Technology. Agriculture, 2022; 12(9): 1457.
[14] Li Y, Xu L Z, Lv L Y, Shi Y, Yu X. Study on modeling method of a multi-parameter control system for threshing and cleaning devices in the grain combine harvester. Agriculture, 2022; 12(9): 1483.
[15] Chen L M, Yi Y H, Wang W X, Zeng Y J, Tan X M, Wu Z M. Innovative furrow ridging fertilization under a mechanical direct seeding system improves the grain yield and lodging resistance of early indica rice in South China. Field Crops Research, 2021; 270: 108184.
[16] Luo X Y, Wu Z F, Fu L, Dan Z W, Yuan Z Q, Liang T. Evaluation of lodging resistance in rice based on an optimized parameter from lodging index. Crop Science, 2022; 62(3): 1318–1332.
[17] Li X W, Lu S C. A comparative discussion on the research progress of dry direct seeding rice and conventional transplanted rice cultivation techniques. Journal of Tianjin Agricultural University, 2021; 28(4): 63–70. (in Chinese)
[18] Ma Z, Zhu Y L, Chen S R, Traore S N, Li Y M, Xu L Z. Field investigation of the static friction characteristics of high-yielding rice during harvest. Agriculture, 2022; 12(3): 327.
[19] Hou M, Ni J H, Mao H P. Effects of airflow disturbance on the content of biochemical components and mechanical properties of cucumber seedling stems. Agriculture, 2023; 13(6): 1125.
[20] Li M Y, Peng G Y, Deng B, Meng G Y. Research progress on vascular bundles in rice. Plant Physiology Journal, 2017; 53(9): 1586–1590. (in Chinese)
[21] Yao Y S, Zhang Z B, Song Y P. Comparison of the growth of Sophora flavescens by direct seeding and transplanting. Chinese Herbal Medicines, 2021; 51(11): 2536–2540. (in Chinese)
[22] Li Z Z, Deng F, Zhang C, Zhu L, He L H, Zhou T. Can relative culm wall thickness' be used to evaluate the lodging resistance of rice? Archives of Agronomy and Soil Science, 2023; 69(6): 934–947.
[23] Wang Q R, Mao H P, Li Q L. Simulation of vibration response of flexible crop stem based on discrete element method. Transactions of the CSAM, 2020; 51(11): 131–137. (in Chinese)
[24] Tang Z, Li Y, Li X Y, Xu T B. Structural damage modes for rice stems undergoing threshing. Biosystems Engineering, 2019; 186: 323–336.
[25] Meng X J, Liang Y G, Zou Z Y, Wang R, Su Y T, Gong X S. Effects of biochar application on rice stem and lodging traits under rice-duck co-breeding. Chinese Journal of Ecology, 2021; 40(10): 3125. (in Chinese)
[26] Gong D K, Zhang X, Yao J P, Dai G J, Yu G X, Zhu Q, et al. Synergistic effects of bast fiber seedling film and nano-silicon fertilizer to increase the lodging resistance and yield of rice. Scientific Reports, 2021; 11(1): 12788.
[27] Chen G H, Deng H B, Zhang G L, Tang W B, Huang H. The correlation of stem characters and lodging resistance and combining ability analysis in rice. Sci. Agric. Sin, 2016; 49: 407–417. (in Chinese)
[28] Huang M S, Li Y M, Chen A Y, Xu L Z. Numerical calculation method of deflection deformation of rice stem. Applied Sciences, 2019; 9(15): 3125.
[29] Berry P M, Spink J, Sterling M, Pickett A A. Methods for rapidly measuring the lodging resistance of wheat cultivars. Journal of Agronomy and Crop Science, 2003; 189(6): 390–401.
[30] Teng X Y, Wang J M, Li Z P, Lin X Y, Sun Q. Research progress on influencing factors and evaluation methods of rice lodging resistance. Fujian Journal of Agricultural Sciences, 2021; 36(10): 1245–1254. (in Chinese)
[31] Wu D, Wu D, Feng H, Duan L F, Dai G X, Liu X. A deep learning-integrated micro-CT image analysis pipeline for quantifying rice lodging resistance-related traits. Plant Communications, 2021; 2(2): 100165.
[32] Wang J, Wu B Z, Kohnen M V, Lin D Q, Yang C C, Wang X W, et al. Classification of rice yield using UAV-based hyperspectral imagery and lodging feature. Plant Phenomics, 2021; 2021: 9765952
[33] Tian M L, Ban S T, Yuan T, Ji Y B, Ma C, Li L Y. Assessing rice lodging using UAV visible and multispectral image. International Journal of Remote Sensing, 2021; 42(23): 8840–8857.
[34] Duan C R, Wang B C, Wang P Q, Wang D H, Cai S X. Relationship between the minute structure and the lodging resistance of rice stems. Colloids and Surfaces B: Biointerfaces, 2004; 35(3-4): 155–158.
[35] Kruszelnicka W, Marczuk A, Kasner R, Batdowska-Witos P, Piotrowska K, Flizikowski J. Mechanical and processing properties of rice grains. Sustainability, 2020; 12(2): 552.
[36] Zargar O, Pharr M, Muliana A. Modeling and simulation of creep response of sorghum stems: Towards an understanding of stem geometrical and material variations. Biosystems Engineering, 2022; 217: 1–17.
[37] Gao H S, Sun Y, Lei X J, Gao Y, Liu H B. Mechanical properties and application of glass fiber reinforced polyurethane composites communication lattice tower. Construction and Building Materials, 2024; 411: 134180.
[38] Hou Y D, Wu L J, Sheng Y H. Solving high-order uncertain differential equations via Adams-Simpson method. Computational and Applied Mathematics, 2021; 40: 1–20.
[39] Hult J. A fourth-order Runge-Kutta in the interaction picture method for simulating supercontinuum generation in optical fibers. Journal of Lightwave Technology, 2007; 25(12): 3770–3775.
[40] Mishnaevsky L. Root causes and mechanisms of failure of wind turbine blades: Overview. Materials, 2022; 15(9): 2959.